Molecular Differences Between Human Thyroid Follicular Adenoma and Carcinoma Revealed by Analysis of a Murine Model of Thyroid Cancer

Marialuisa Sponziello, Elisa Lavarone, Enrico Pegolo, Carla Di Loreto, Cinzia Puppin, Marika A. Russo, Rocco Bruno, Sebastiano Filetti, Cosimo Durante, Diego Russo, Antonio Di Cristofano, and Giuseppe Damante

Dipartimento di Medicina Interna e Specialità Mediche (M.S., S.F., C.D.), Università di Roma "Sapienza," 00161 Roma, Italy; Dipartimento di Scienze Mediche e Biologiche (E.L., E.P., C.D.L., C.P., G.D.), Università di Udine, and Azienda Ospedaliero-Universitaria "S. Maria della Misericordia" (C.D.L., G.D.), 33100 Udine, Italy; Department of Developmental and Molecular Biology (M.A.R., A.D.C.), Albert Einstein College of Medicine, Bronx, New York 10461; Unità di Endocrinologia (R.B.), Ospedale di Tinchi-Pisticci, 85100 Matera, Italy; and Dipartimento di Scienze della Salute (D.R.), Università di Catanzaro, 88100 Catanzaro, Italy

Mouse models can provide useful information to understand molecular mechanisms of human tumorigenesis. In this study, the conditional thyroid mutagenesis of *Pten* and *Ras* genes in the mouse, which induces very aggressive follicular carcinomas (FTCs), has been used to identify genes differentially expressed among human normal thyroid tissue (NT), follicular adenoma (FA), and FTC. Global gene expression of mouse FTC was compared with that of mouse normal thyroids: 911 genes were found deregulated ± 2-fold in FTC samples. Then the expression of 45 deregulated genes in mouse tumors was investigated by quantitative RT-PCR in a first cohort of human NT, FA, and FTC (discovery group). Five genes were found significantly down-regulated in FA and FTC compared with NT. However, 17 genes were found differentially expressed between FA and FTC: 5 and 12 genes were overexpressed and underexpressed in FTC vs FA, respectively. Finally, 7 gene products, selected from results obtained in the discovery group, were investigated in a second cohort of human tumors (validation group) by immunohistochemistry. Four proteins showed significant differences between FA and FTC (peroxisomal proliferator-activated receptor-γ, serum deprivation response protein, osteoglycin, and dipeptidase 1). Altogether our data indicate that the establishment of an enriched panel of molecular biomarkers using data coming from mouse thyroid tumors and validated in human specimens may help to set up a more valid platform to further improve diagnosis and prognosis of thyroid malignancies. (***Endocrinology*** **154: 3043–3053, 2013)**

A major notion of tumorigenesis is that human cancers such as those arising from colon, breast, and lung evolve toward aggressiveness in a multistep process. According to this model, characteristic molecular alterations appear in benign, nonaggressive lesions and accumulate during progression (1, 2). Thus, molecular alterations shared by carcinomas and benign counterparts would represent early events of transformations, whereas those present only in aggressive forms would be responsible for progression. Identification of these latter ones, in addition to shedding light on the mechanisms responsible for advances in aggressiveness, could be used as markers for clinical management (ie, diagnosis, prognostic stratification, and selection of therapeutic targets for molecular therapy) (3, 4).

Tumor progression also may occur in neoplasms derived from the thyroid follicular cells. Histologically, these tumors consist of differentiated thyroid cancer, including

ISSN Print 0013-7227 ISSN Online 1945-7170
Printed in U.S.A.

Received January 8, 2013. Accepted June 4, 2013.
First Published Online June 10, 2013

Abbreviations: Ct, cycle threshold; DPEP1, dipeptidase 1; FA, follicular adenoma; FDR, false discovery rate; FTC, follicular thyroid cancer; NT, normal thyroid tissue; OGN, osteoglycin/mimecan; PAX8, paired box transcription factor 8; PPAR, peroxisomal proliferator-activated receptor; PTC, papillary thyroid cancer; PTEN, phosphatase and tensin homolog deleted from chromosome 10; SDPR, serum deprivation response protein.

papillary thyroid cancer (PTC) and follicular thyroid cancer (FTC) and undifferentiated cancer (5, 6). Several lines of evidence indicate that FTC would initiate from a follicular adenoma (FA) (7, 8). In contrast, no premalignant lesion for PTC has been clearly identified.

Several specific genetic alterations have been found in thyroid tumors (9). The *BRAF* V600E mutation and *RET-PTC* rearrangements are common in PTC, whereas *RAS* mutations and the *PAX8-PPARγ* rearrangement are common in FTC and, at a much lower frequency, in FA. In addition to genetic modifications, alteration of expression levels for critical cancer genes has been noticed in thyroid cancer. For example, various data indicate that in thyroid cancer *PTEN* expression is reduced (10–12). Altogether, mutations or altered expression of these oncogenes/tumor suppressor genes induce activation of 2 major cancer-related signaling cascades: the MAPK and the phosphatidylinositol 3-kinase/Akt pathways (13–15).

Identification of molecular alterations of thyroid cancer may have important consequences: for example, detection of genetic alterations allows improving diagnostic predictions. One of the most difficult tasks that physicians face in clinical practice is to preoperatively distinguish FA from FTC. Currently this differential diagnosis relies primarily on cytology. However, the latter fails to effectively discriminate between these 2 lesions in up to 30% of cases. In the last years, several candidate markers for thyroid cancer have been investigated for the diagnostic assessment of thyroid cytological samples. Gene mutations and the expression of mRNA have been tested to this purpose (9, 16). Although both these approaches improved the accuracy of cancer detection, they still hold some limits in term of sensitivity and specificity, respectively. Therefore, there is a clinical need for new reliable preoperative molecular markers able to correctly classify these tumors. In this regard, by introducing in the mouse specific genetic alterations found in human cancer, relevant models of thyroid tumorigenesis have been generated and are now used as an invaluable tool to understand the molecular bases of tumor progression as well as to test novel molecular targeted therapies (17).

Using a mouse model in which conditional mutations have been specifically introduced in thyroid follicular cells, it has been shown that the simultaneous activation of the *K-Ras* oncogene and inactivation of the *Pten* tumor-suppressor gene induces very aggressive thyroid follicular carcinomas (18). These mutants do not develop hypothyroidism or high TSH. Although in these mice, in contrast to human pathology, genetic alterations are already present before birth, they represent an excellent animal model of aggressive thyroid cancer. In the present study, we have first used this mouse model to identify a panel of genes with differences in their expression between carcinoma and normal thyroid tissue; subsequently this information was used to select a pattern of genes that were investigated in a series of human tissues including normal thyroid, FA and FTC. Several genes differentially expressed between FA and FTC have been identified, and for some of them, additional validation of the data using immunohistochemistry was performed.

Materials and Methods

Mouse tissue expression profiling

Three pools of 3–5 wild-type and single mutant thyroids and 3 individual, fresh-frozen, histologically verified tumor samples from $Pten^{thyr-/-}$,$Kras^{G12D}$ mice were randomly selected. Tumor fragments and thyroid glands were subjected to total RNA isolation using TRIzol reagent (Invitrogen, Carlsbad, California) followed by further purification with the RNAeasy kit (QIAGEN, Venlo, The Netherlands). Total RNA quality was verified using the Agilent Bioanalyzer 2100 (Berks, United Kingdom). Microarray hybridization was performed at the Albert Einstein Genomics Facility using Affymetrix Mouse Gene 1.0 arrays (Santa Clara, California). Normalization and background subtraction were performed with multi-array average, using the oligo package of Bioconductor (Seattle, Washington). Gene selection was performed using the limma package. Raw *P* values were corrected for multiple testing using a false discovery rate (FDR) of less than 0.05. Microarray data were deposited in Gene Expression Omnibus (accession number GSE30427).

All experimental procedures made with mice have been conducted in accord with accepted standard of animal care.

Canonical pathway analysis

Canonical pathways analysis identified the pathways from the Ingenuity Pathways Analysis library of canonical pathways that were most significant to the data set. Molecules from the data set that met the ±2-fold cutoff with a FDR of less than 0.05 and were associated with a canonical pathway in Ingenuity's Knowledge Base were considered for the analysis.

The significance of the association between the data set and the canonical pathway was measured in 2 ways: 1) a ratio of the number of molecules from the data set that map to the pathway divided by the total number of molecules that map to the canonical pathway; and 2) a Fisher's exact test was used to calculate a *P* value determining the probability that the association between the genes in the data set and the canonical pathway is explained by chance alone.

Human thyroid tissues

Two different independent groups of human thyroid tumors were used. The first (discovery group) was used to identify differential gene expression between normal thyroid tissue (NT), FA, and FTC in terms of mRNA levels, starting from mouse data. The second (validation group) was investigated by immunohistochemistry, starting from the data obtained with the discovery group.

For the discovery group, thyroid tissues were obtained at thyroidectomy from 14 patients with FTC and from 50 patients with

FA. The former group included 8 patients with FTC manifesting only capsular invasion (minimally invasive FTC) and 6 patients with FTC displaying vascular invasion (invasive FTC). The samples were snap frozen in liquid nitrogen and stored at −80°C. As control, we used nonnodular tissues from 8 patients subjected to surgery for the removal of benign thyroid nodules.

For the validation group, a series of 27 FTCs and 26 FAs were selected from the files of the Institution of Anatomic Pathology of the University of Udine; the most representative block of each lesion was retrieved from the archive.

All samples have been collected from areas having mild to moderate iodine deficiency.

All samples were diagnosed by referral pathologists of institutions and then reviewed by a single experienced pathologist, thus including only patients with a confirmed diagnosis (follicular carcinoma or follicular adenoma) and excluding specimens with the presence of normal tissue.

The study was approved by the local medical ethics committee. Before surgery, each study participant provided written, informed consent to the collection of fresh thyroid tissue for genetic studies.

Molecular analysis of human tissues

Total RNA was extracted from human fresh frozen tissue samples using an RNeasy minikit (QIAGEN) according to the manufacturer's instructions. Two micrograms of total RNA were used for cDNA synthesis using 200 U Moloney murine leukemia virus reverse transcriptase and 600 ng random hexamers (Life Technologies, Paisley, United Kingdom) in a reaction volume of 20 μL. Gene expression profiles were assessed by real-time PCR using microfluidic cards (Taqman low density arrays; Life Technologies) in an ABI PRISM 7900HT sequence detection system (Life Technologies). Each Taqman low-density array was configured with specific Taqman gene expression assays (Life Technologies) for 48 genes (selected by previous microarray results) by 1 replicate per biological sample. Three housekeeping genes (*GAPDH*, *GUSB*, and *HRPT1*) were included to normalize the raw data.

The reaction set -up, briefly, consisted of 100 ng of each cDNA template sample made up to 50 μL with ribonuclease-free water and equal amounts of 2× Taqman Universal PCR Master Mix II (Life Technologies). One hundred microliters of each sample-specific PCR reaction mix were loaded into each of the 8 ports of the array. The Taqman array was centrifuged twice for 1 minute each at 1200 rpm to distribute the cDNA samples to the reaction wells. The card was then sealed to isolate the wells, and PCR amplification was performed using an ABI PRISM 7900HT sequence detection system (Life Technologies). Thermal cycler conditions were as follows: 10 minutes at 95°C, 15 seconds at 95°C, and 1 minute at 60°C for 40 cycles. Cycle threshold (Ct) values, defined as the point at which the fluorescence rises above the background fluorescence, were calculated with SDS 2.3 software (Life Technologies), and the detectability threshold was set to 33. Data analysis was carried out using RQ Manager 1.2 software (Life Technologies). Results were determined by the 2-ΔΔCt method (19) and expressed as relative expression normalized to a calibrator sample (normal tissues). Hotspot *H-RAS*, *K-RAS*, and *N-RAS* mutations (codons 12, 13, and 61) were identified by sequence analysis of products obtained by RT-PCR amplification of exons 2 and 3.

All PCR reactions and sequencing were repeated at least twice to confirm the presence of a mutation. Primers are shown in Supplemental Table 1, published on The Endocrine Society's Journals Online web site at http://endo.endojournals.org. Quantitative RT-PCR analysis to evaluate phosphatase and tensin homolog deleted from chromosome 10 (PTEN) mRNA levels was performed as previously described (20). A 25-μL reaction mixture containing 5 μL cDNA template, 12.5 μL Taqman Universal PCR master mix (Applied Biosystems, Foster City, California), and 1.25 μL primer probe mixture was amplified using the following thermal cycler parameters: incubation at 50°C for 2 minutes and denaturation at 95°C for 10 minutes and then 40 cycles of the amplification step (denaturation at 95°C for 15 s and annealing/extension at 60°C for 1 min). The ΔCt method, by means of the SDS software (Applied Biosystems), was used to calculate the mRNA levels. Oligonucleotide primers and probes for *PTEN* are described in Supplemental Table 1. Oligonucleotide primers and probes for the endogenous control, glyceraldehyde-3-phosphate dehydrogenase, were purchased from Applied Biosystems as Assays-on-Demand gene expression products.

Immunohistochemistry

On each case of the validation group, immunohistochemical stains for peroxisomal proliferator-activated receptor (PPAR)-γ, secreted frizzled-related protein 1, serum deprivation response protein (SDPR), ephrin receptor A5, dipeptidase 1 (DPEP1), fibulin-1, and osteoglycin/mimecan (OGN) were performed. In brief, 4-μm sections mounted on SuperFrost Plus slides (Menzel-Gläser, Braunschweig, Germany) were pretreated in a water bath as detailed in Supplemental Table 2. After quenching the endogenous peroxidase using a solution of 0.3% hydrogen peroxide in methanol, the slides were placed in the DAKO Autostainer Link 48 and incubated with the primary antibodies followed by the DAKO EnVision FLEX antibody detection system (DAKO Corp, High Wycombe, United Kingdom). Diaminobenzidine was used as a chromogen, and Gill's hematoxylin was applied for counterstaining. Appropriate positive and negative tissue controls were run for each antibody. A brown color identified the positive cells.

All the immunohistochemical stains were evaluated by the same pathologist that assessed the percentage of immunoreactive tumor cells and the intensity of the staining graded in low (score 1), moderate (score 2), or strong (score 3). A final semiquantitative score was then calculated by multiplying the percent staining by the intensity level.

Results

Differential gene expression in mouse tissues

To gain insight into the molecular characteristics of the aggressive FTCs developed by $Pten^{thyr-/-}$,$Kras^{G12D}$ compound mutants, we performed genome-wide expression profiling using the Affymetrix platform on thyroids from 3-month-old control, single mutants and double mutant-induced mice tumors.

As predicted by the inability of thyroid-specific *Kras* activation to yield an overt phenotype (18), a heat map

including all probes with more than a 2-fold change across any of the 4 groups showed that *Kras*^{G12D} thyroids cluster together with those of wild-type mice (Figure 1). On the other hand, significant differences were apparent between the transcriptomes of control and *Pten*$^{thyr-/-}$ thyroids. Moreover, the profile of *Pten*$^{thyr-/-}$,*Kras*^{G12D} FTCs was strikingly different from that of *Pten*$^{thyr-/-}$ mice. These data strongly suggest that the molecular events leading to the development and maintenance of FTC in the compound mutants are unique for each tumor and that characterization of these changes could uncover clinically relevant pathways and targets.

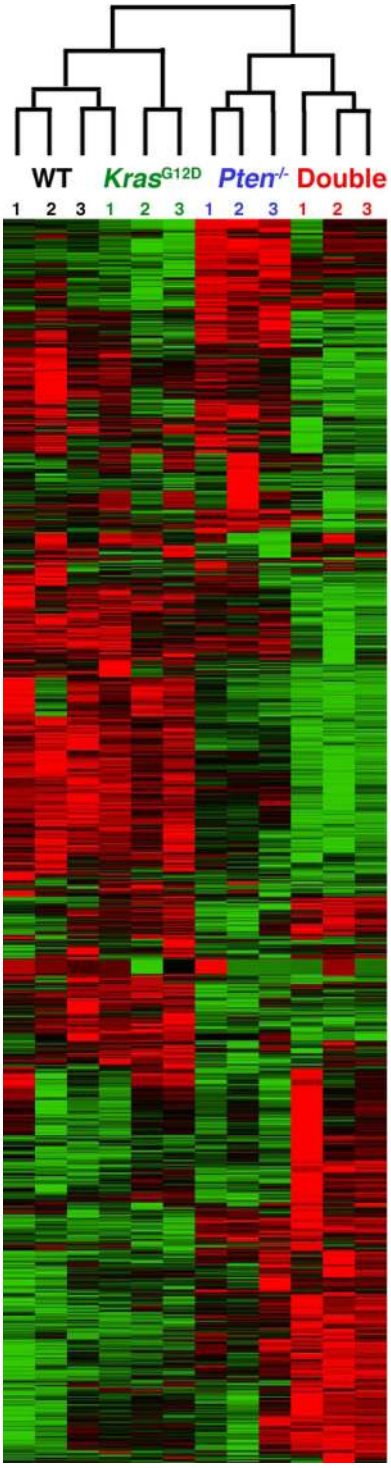

Figure 1. Heat map of gene expression in wild-type and conditional mutant mice. Each column indicates gene expression of a pool of 3–5 wild-type and single-mutant thyroids and 3 individual, fresh-frozen, histologically verified tumor samples from *Pten*$^{thyr-/-}$,*Kras*^{G12D} mice. Green and red signals indicate low and high gene expression, respectively.

Overall, using a stringent FDR of 5%, 911 genes were found deregulated ±2-fold in FTC samples, compared with wild-type thyroids (287 up and 624 down) (deposited in the Gene Expression Omnibus database). To identify biological processes significantly impacted by the development of the more aggressive phenotype, we performed canonical pathway enrichment using Ingenuity Pathway Analysis. A significant enrichment was observed, among others, in pathways involved in leukocyte recruitment and function, epithelial-mesenchymal transition, and thyroid cancer signaling (Table 1). The top 50 up-regulated and down-regulated genes in the tumors developed by *Pten*$^{thyr-/-}$,*Kras*^{G12D} compound mutants compared with normal thyroid are listed in Table 2.

Differential gene expression in human thyroid tissues of the discovery group

Based on data obtained in the mouse model, 45 genes were selected to be investigated in human thyroid tissues (Supplemental Table 3). Expression of these genes was evaluated by quantitative RT-PCR using the Taqman low-density array system in 8 NTs, 50 FAs, and 14 FTCs. In a first analysis, the mRNA expression levels of NT, FA, and FTC were evaluated and compared among the 3 groups. Considering a cutoff of at least 30% difference above or below the values detected in NT, expression of 22 of 45 genes changed in the same direction in FA and FTC (Supplemental Table 4). In particular, among the genes overexpressed in both FA and FTC compared with NT, only *LCN2* shows a statistically significant difference between NT and FTC. Instead, among the genes underexpressed in both FA and FTC, 5 of them show significant difference compared with NT, namely *FABP5*, *FBL1*, *OGN*, *PTPRD*, and *SRDSA1* (Figure 2). The similar deregulation of gene expression detected in FAs and FTCs supports the notion that these 2 neoplasms share common tumorigenic pathways.

We then focused on genes differentially expressed between FA and FTC. Seventeen genes were identified: 5 and 12 genes are overexpressed and underexpressed in FTC vs FA, respectively (Figure 3). Interestingly, 11 of these genes were also significantly deregulated when comparison with NT was performed (Supplemental Table 4).

Table 1. Top 25 Deregulated Pathways Identified in Mouse FTCs, Using the Ingenuity Pathways Analysis System

Ingenuity Canonical Pathways	*P* Value	Ratio
iCOS-iCOSL Signaling in T helper cells	.00001	0.14
Primary immunodeficiency signaling	.00002	0.16
LXR/RXR activation	.00004	0.13
T cell receptor signaling	.00005	0.15
Hepatic fibrosis/hepatic stellate cell activation	.00005	0.14
Complement system	.00010	0.23
Thyroid cancer signaling	.00021	0.21
Calcium-induced T lymphocyte apoptosis	.00034	0.14
Pathogenesis of multiple sclerosis	.00054	0.44
B cell development	.00072	0.18
CCR5 signaling in macrophages	.00115	0.11
Communication between innate and adaptive immune cells	.00195	0.09
Atherosclerosis signaling	.00219	0.10
Factors promoting cardiogenesis in vertebrates	.00234	0.13
Eicosanoid signaling	.00288	0.11
Hematopoiesis from pluripotent stem cells	.00302	0.10
cAMP-mediated signaling	.00324	0.10
Nicotine degradation II	.00331	0.10
Mitotic roles of polo-like kinase	.00372	0.13
CD28 signaling in T helper cells	.00468	0.10
Leukocyte extravasation signaling	.00562	0.09
Protein kinase A signaling	.00617	0.08
Nitric oxide signaling in the cardiovascular system	.00646	0.10
Estrogen-mediated S-phase entry	.00891	0.18
IL-12 signaling and production in macrophages	.01072	0.08

Abbreviations: iCOS, inducible costimulator; iCOSL, inducible costimulator ligand; LXR, liver X receptor; RXR, retinoid X receptor; CCR5, chemochine receptor 5.

When we analyzed the differential gene expression profile between minimally invasive and invasive FTCs, the latter group displayed lower *AOC3* and *GPX3* mRNA levels and higher *TIMP1*, *TPX2*, and *KIF20A* mRNA levels (Supplemental Table 5).

Our FTC cohort was further screened for the presence of oncogenic *RAS* mutations. Five of 14 FTCs show the presence of 1 mutant *RAS* allele. Thus, the gene profile results were further revisited, taking into account the presence of the *RAS* mutation in a subgroup of samples. Among the 45 genes selected from the mouse study, *CCND1*, *ETV5*, and *PTPRD* display significant difference among the 2 groups (Figure 4A). Expression of all 3 genes is up-regulated in the FTC-bearing *RAS* mutation. *PTEN* gene expression was evaluated in all human specimens (Figure 4B). Levels of *PTEN* mRNA in FTCs are lower than in NT and, although a certain degree of overlap, are also lower than in FAs. No difference in *PTEN* gene expression was detected in FTC containing or not *RAS* mutations.

Immunohistochemistry in human thyroid tissues of the validation group

To test whether results obtained in the discovery group could be replicated in a second series of tumors and whether mRNA expression data would correspond to altered protein expression, a second group of patients' tumor tissues (validation group) was investigated by immunohistochemistry. This series comprises 26 FAs and 27 FTCs. Seven proteins whose genes are differentially expressed between FA and FTC were selected for immunohistochemical evaluation. Quantitation of the immunohistochemical signal was obtained by computing percentage of cell positivity and intensity of signal. Table 3 summarizes the results obtained. Four proteins show significant differences between FA and FTC. However, only for 3 of them (PPARγ, SDPR, and OGN), the changes detected by immunohistochemistry parallel those obtained by quantitative RT-PCR (PPARγ values are higher in FTCs than in FAs, whereas SDPR and OGN values are higher in FAs than in FTCs). DPEP1, instead, shows an opposite behavior: protein levels are higher in FTCs, whereas the mRNA levels are higher in FAs. Representative images of PPARγ, SDPR, OGN, and DPEP1 staining in FAs and FTCs are shown in Figure 5. Thus, using 2 different groups of patients, 3 of 7 genes show, in terms of mRNA and protein levels, the same trend of expression when FA is compared with FTC.

Discussion

Molecular features of animal models of cancer may help in the identification of differences existing between human normal and tumor tissues. Such information can be, in turn, of relevance for diagnostic and prognostic purposes as well as for the development of novel therapeutic ap-

Table 2. Top 50 Genes Deregulated in Mouse FTCs, Ranked by Expression Level

Up			Down		
Mouse Gene	**Fold Change**	***P* Value**	**Mouse Gene**	**Fold Change**	***P* Value**
Lipk	29.8	2.36E-07	*Cyp2e1*	0.018	5.23E-19
Moxd1	11.9	1.78E-10	*Ucp1*	0.034	6.89E-08
Mia	11.2	1.57E-11	*Pon1*	0.043	5.62E-17
Lcn2	10.2	5.05E-05	*Tmem45b*	0.047	1.21E-10
Gng4	7.7	5.41E-06	*Retn*	0.049	4.80E-19
Fam84a	7.5	2.35E-07	*Ca3*	0.050	1.17E-05
Chi3l1	7.1	1.84E-04	*Cox8b*	0.055	3.27E-09
Bcas1	6.8	2.82E-10	*Penk*	0.056	1.50E-14
Kiaa1324l	6.0	6.73E-07	*Inmt*	0.056	1.52E-16
Ddah1	5.8	2.86E-09	*Adipoq*	0.060	2.12E-12
Dcx	5.6	4.37E-14	*Cidec*	0.061	2.18E-12
Sftpb	5.6	5.03E-05	*Cidea*	0.061	4.20E-12
1700049E17Rik1	5.3	6.69E-10	*Cxcl13*	0.064	1.22E-10
Camk1g	5.1	2.84E-05	*Adh1c*	0.066	9.83E-12
Rlbp1	5.1	1.14E-07	*Aqp7*	0.075	9.46E-11
St6gal1	5.1	2.82E-09	*Fmo1*	0.077	2.49E-10
Fam178b	5.1	5.70E-14	*Pck1*	0.079	8.67E-11
Atp6v0d2	5.1	9.65E-07	*Cfd*	0.084	1.06E-15
Timp1	4.6	1.27E-05	*Cxcl10*	0.087	8.42E-08
Ttc39c	4.6	9.27E-09	*Plin1*	0.089	1.26E-13
Bbox1	4.6	8.58E-10	*Lgals12*	0.095	3.02E-10
Lppr1	4.5	2.50E-13	*Rbp4*	0.097	4.16E-08
Fam174b	4.3	5.58E-06	*Slc36a2*	0.100	7.82E-13
Gm16440	4.3	1.39E-09	*Bpifa1*	0.100	2.34E-04
Ggt5	4.3	2.07E-09	*Satb1*	0.103	2.41E-04
Srd5a1	4.2	1.72E-03	*Kl*	0.105	7.13E-07
Nkx2–2	4.2	2.11E-07	*Psca*	0.107	1.97E-04
Slco4c1	4.2	3.56E-05	*Themis*	0.108	5.46E-03
Agr2	4.2	5.04E-04	*Lpl*	0.109	1.62E-08
Cml3	4.1	8.26E-05	*Scg3*	0.109	3.43E-15
Kif20a	4.0	2.06E-07	*Mup1*	0.110	3.36E-05
Cndp1	3.9	5.63E-10	*Abcd2*	0.111	7.56E-15
Plekhs1	3.9	2.59E-08	*Nrg4*	0.113	7.31E-18
Cdh4	3.8	6.64E-07	*Leprel1*	0.115	2.05E-10
Cdk1	3.8	9.81E-07	*Cxcl11*	0.116	1.24E-07
Tmem150c	3.8	3.02E-13	*Pcsk2*	0.120	4.35E-14
Acnat1/Acnat2	3.8	7.02E-07	*Cd36*	0.126	1.52E-06
Atp6v0a4	3.7	2.26E-09	*Fmo2*	0.127	5.93E-09
Thbs4	3.7	1.16E-03	*Apod*	0.129	3.54E-09
St8sia6	3.6	8.93E-05	*Mamdc2*	0.130	7.67E-07
Serpine1	3.6	3.13E-05	*Ccr9*	0.133	8.63E-03
Anln	3.6	3.66E-07	*Scgb1a1*	0.136	1.39E-03
Cldn10	3.6	2.07E-04	*Cd8b*	0.137	3.89E-03
Smoc2	3.6	1.44E-06	*Pde3b*	0.141	3.22E-08
Sphk1	3.6	2.68E-05	*B3galt2*	0.144	1.46E-13
Hhatl	3.4	4.61E-04	*Retnla*	0.145	1.85E-04
C2orf40	3.4	1.75E-05	*Rgs7*	0.146	2.93E-14
Sytl5	3.4	5.80E-04	*Atp1a2*	0.146	1.13E-08
Rny1	3.4	6.79E-03	*Anpep*	0.148	1.42E-10
Ces1e	3.3	8.78E-09	*Casr*	0.149	1.44E-08

proaches. The relevance of mouse models to a better knowledge of follicular and papillary human thyroid cancer has been recently pointed out (17). In the present research, to gain insights into the molecular features of FTC, we started our study from a mouse model in which activating mutation of the *Kras* oncogene and the deletion of the oncosuppressor *Pten* are simultaneously present (18).

In this animal model, each of these 2 mutations alone is unable to induce transformation of thyroid follicular cells; however, their concurrent activation induces highly aggressive follicular carcinomas already at 12 weeks of age (18). In effect, loss of *Pten* alone induces follicular adenomas in two thirds of female mice by 10 months of age (21). However, to focus on the early phase of malignant

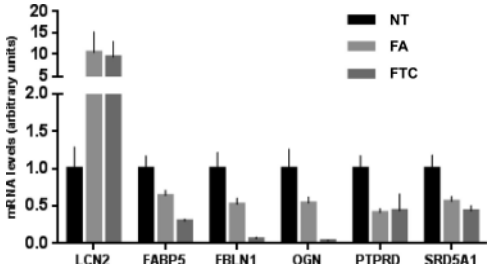

Figure 2. Gene expression in the human discovery group: mRNA levels of genes differentially expressed in FA and FTC vs NT. Levels of mRNAs were evaluated by Taqman microfluidic card as described in *Materials and Methods*. Each column indicates the mean value ± SEM of 8 NT, 57 FA, and 14 FTC. Mean values of NT were arbitrarily expressed as 1.

transformation, 12-week-old animals were compared, and at this age, *Pten*$^{thyr\ -/-}$ mice do not display adenomas. Consistent with these phenotypic data, in a microarray analysis, mouse FTC tissues show dramatic differences compared with both normal and single mutant tissues.

Starting from genes that are differentially regulated in mouse FTC compared with normal thyroid tissue, 45 genes have been selected to investigate human tumors, and their mRNA levels were investigated in human NT, FAs, and FTCs. The choice of these 45 genes was done by combining 3 criteria: 1) the level of differential expression in mouse FTC compared with mouse normal thyroid; 2) the possibility to have the specific probe in the micro fluidic card (see *Materials and Methods*); 3) the involvement in cell transformation. This latter criterion was based on searching the PubMed database (http://www.ncbi.nlm.nih.gov/pubmed) using as key words the gene name and the word cancer. Interestingly, when double-mutant mice were compared with either wild-type or *Pten*$^{thyr-/-}$ mice, for 44 of these 45 genes, the modification of expression occurs in the same direction (Supplemental Table 6). These data support the notion that in 12-week-old animals, with respect to genes deregulated in double-mutant mice, wild-type and *Pten*$^{thyr-/-}$ mice have very similar

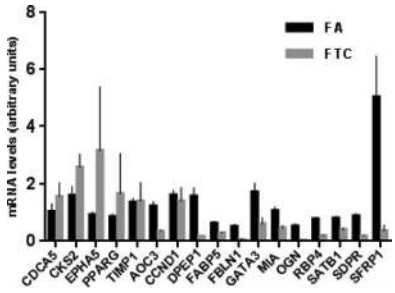

Figure 3. Gene expression in the human discovery group: mRNA levels of genes differentially expressed between FA and FTC. Levels of mRNAs were evaluated by Taqman microfluidic card as described in *Materials and Methods*. Each column indicates the mean value ± SEM of 57 FA and 14 FTC. mRNA levels are expressed as fraction of values found in NT, considered arbitrarily as 1.

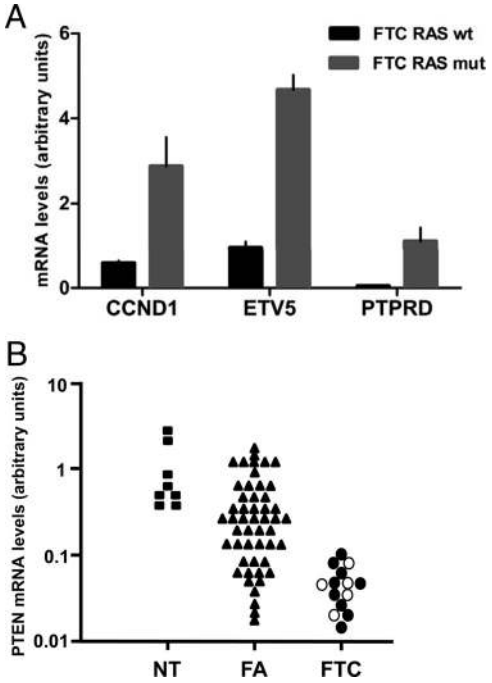

Figure 4. A, Differentially expressed genes between FTC with and without *RAS* mutation. Black and gray columns indicate the mean value ± SEM of FTC with (5 cases) and without (9 cases) *RAS* mutations, respectively. mRNA levels are expressed as fraction of values found in NT, considered arbitrarily as 1. B, *PTEN* gene expression in specimens of the discovery group. Each symbol indicates *PTEN* gene expression in a single specimen. Black squares, NT; black triangles, FA; black circles, FTC without *RAS* mutations; white circles, FTC with *RAS* mutations. *PTEN* mRNA levels are expressed as a fraction of the mean value of NT specimens.

expression patterns. Among the 45 genes, 17 show a significant mRNA level difference between human FAs and FTCs in the discovery group, and 7 of these were further investigated by immunohistochemistry (thus evaluating levels of their protein products) in a validation group. These 7 genes have been chosen by combination of 2 criteria: a significant difference between FAs and FTCs and involvement in cell transformation. For 4 genes the immunohistochemical signal was significantly different among FA and FTC: PPARγ, OGN, SDPR, and DPEP1.

Table 3. Quantification of Immunohistochemical Signals

Protein	FA (Mean ± SD)	FTC (Mean ± SD)	*P* Value
PPARγ	13.38 ± 26.17	47.33 ± 79.45	.0433
SFRP1	134.8 ± 73.99	147.7 ± 72.17	.5646
SDPR	50.62 ± 56.24	20.0 ± 11.78	.0288
EPHA5	41.13 ± 36.71	28.89 ± 36.87	.2965
DPEP1	3.57 ± 11.75	20.0 ± 2.88	.0486
FBL1	24.38 ± 34.61	36.04 ± 40.02	.2932
OGN	63.31 ± 80.68	24.96 ± 41.96	.0337

Abbreviations: EPHA5, ephrin receptor A5; FBL1, fibulin-1; SFRP1, secreted frizzled-related protein 1.

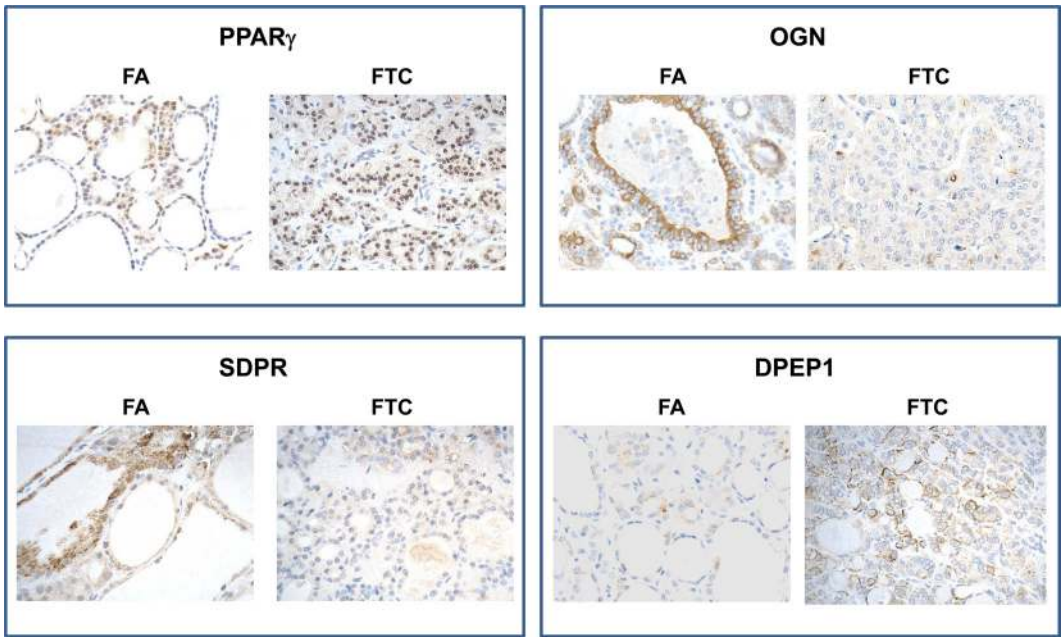

Figure 5. Immunohistochemical analysis of validation group tumors. Each panel shows representative cases of differential staining between FA and FTC for PPARγ, OGN, SDPR, and DPEP1 proteins. In all panels positivity is indicated by brown staining.

PPARγ is already known to be involved in the generation/progression of follicular tumors. In fact, the t (2, 3)(q13,p25) translocation that determines the expression of the fusion protein paired box transcription factor 8 (PAX8)-PPARγ (8, 23) is present in FTC and, although with a lower frequency, in FA. The fusion with PAX8 suppresses the wild-type function of PPARγ, considered an inhibitor of cell growth and a promoter of differentiation (24, 25). Moreover, the fusion protein is overexpressed compared with wild-type PPARγ because it is subjected to the transcriptional control normally acting on the *PAX8* gene, which is active in thyroid follicular cells (26). It is noteworthy that, although in mouse tumors PPARγ mRNA levels are lower in FTC than in normal tissues, in human tissue specimens, PPARγ mRNA levels resulted higher in FTC than in FA and NT. However, in our series of human tumors, this difference is due to the presence of the *PAX8-PPARγ* translocation. In fact, when in the discovery group human cases containing the *PAX8-PPARγ* translocation are excluded, PPARγ mRNA levels are significantly reduced in FTC compared with FA and NT, and a similar behavior is detected also in the validation group. Thus, our expression data support the possibility that the wild-type PPARγ and the PAX8-PPARγ fusion proteins play an opposite role in the transformation process with oncosuppressor and oncogenic functions, respectively. Functional data are, however, required to confirm this hypothesis.

OGN belongs to a class of proteoglycans), the small leucine-rich proteoglycans that are secreted into the extracellular matrix (27). In vitro studies suggest that osteoglycin may play a role in cellular growth control, as judged by ability of growth factors and cytokines to modulate its mRNA expression in corneal keratocytes and vascular smooth muscle cells (28, 29). OGN mRNA is absent or at low levels in most cancer cell lines and tumors (30). Wang et al (31), for example, demonstrated that OGN expression is down-regulated in colorectal adenoma and cancer when compared with the normal tissue. Our data would indicate that a decrease of OGN expression parallels thyroid tumor progression. In fact, *OGN* mRNA levels are the highest in NT and the lowest in FTC.

SDPR is a phosphatidylserine-binding protein member of the caveolae family protein, which are specialized invaginations of the plasma membrane implicated in many cellular functions including signal transduction, lipid regulation, endocytosis, and tumorigenesis (32). An analysis of SDPR expression in human tissues has revealed an almost ubiquitous expression, with the highest levels found in the heart and lung (33). In tumors, SDPR is suppressed in the breast, kidney, and prostate malignancies (34). Together with these data, our finding supports the potential use of SDPR as a tumor biomarker also for thyroid neoplasia.

DPEP1 is a zinc-dependent metallopeptidase that hydrolyzes a variety of dipeptides and is involved in glutathione metabolism (35). The relationship between the expression of DPEP1 and the initiation/progression of cancer appears quite complex. It has been shown that DPEP1 is highly expressed in colon tumors compared with

matched normal mucosa (36). Moreover, Toiyama et al (37) showed that DPEP1 expression is very low in normal colonic mucosa, but it is high in colorectal cancer specimens and is negatively correlated with parameters of pathological aggressiveness such as lymph node metastasis, distant metastasis, and poor prognosis. However, in Wilms' tumor and breast lobular carcinoma, DPEP1 shows decreased expression compared with normal tissues (38, 39). Thus, the down- or up-regulation of DPEP1 expression seems dependent on the cell type of tumor origin. Our immunohistochemical data would suggest that DPEP1 expression increases along the FA to FTC progression. Because DPEP1 is a membrane-bound dipeptidase, it may play a role in the degradation of surrounding extracellular matrix components, which would increase the ability of tumor cells to invade from the primary site through the extracellular matrix. The reasons for the discrepancy present in our study related to DPEP1 expression (protein levels are higher in FTC than in FA, but the reverse phenomenon is observed for mRNA levels) are not clear. However, it might be due to differences of translational efficiency of the DPEP1 mRNA between FTC and FA. In fact, by quantifying the regulation of global gene expression, Schwanhäusser et al (40) have recently shown that the cellular abundance of proteins is predominantly controlled at the translational level.

Except for PPARγ, further studies are required to reveal a functional role in thyroid tumorigenesis of the additional proteins identified by immunohistochemistry as differentially expressed between FA and FTC (OGN, SDPR, and DPEP1) in addition to that of potential diagnostic biomarkers.

By using global gene profiling, several genes differentially expressed between benign and malignant thyroid nodules have been identified in the last few years (41–49). However, none of the identified genes is significantly modified among the 45 genes that have been selected for analysis in humans, with the exception of the *CKS2* and *SDPR* genes. In fact, Borup et al (49) have shown that *CKS2* and *SDPR* are over- and underexpressed in FTC compared with FA, respectively. These results are very similar to those obtained in the present study (see Supplemental Table 4). In a meta-analysis in which various studies of thyroid cancer profiling have been analyzed together, several genes have been identified as differentially expressed between malignant thyroid nodules with respect to benign ones or normal tissues (50). Among them *ETV5* and *TIMP1* are included in our group of 45 selected for human investigation; however, in our cohort only *TIMP1* shows a significant differential expression between FTC and FA (Supplemental Table 4).

Discovery of novel molecular biomarkers may not only provide additional tools for the prognosis of patients with thyroid cancer but also be helpful contribution for the diagnosis of uncertain lesions. It is well established the role of fine-needle aspiration cytology of thyroid nodules for assessment of the morphological features critical to predict malignancy and therefore to decide whether to perform surgical treatment (51). However, up to 30% of aspirations gives indeterminate cytological findings (52), usually requiring thyroid gland removal and histological examination to distinguish benign from malignant lesions. After surgery, it is found that most of these patients (almost 80%) have a benign disease. In these cases, therefore, surgery was unnecessary and potentially dangerous considering that surgical removal of thyroid cancer has a 2%–10% rate of long-term morbidity (53, 54). This picture is almost invariably associated with the occurrence of a follicular histotype. For these reasons in the last several years, various classifiers based on the molecular features of thyroid nodules, detectable in the DNA and RNA extracted from the cytoaspirates, have been proposed (44, 55, 56).

To date, the most successful mutational panel allowing the preoperative detection of malignancies in thyroid nodules includes *BRAF* and *RAS* mutations and *RET/PTC*, *PAX8-PPAR*$\gamma\gamma$, and *TRK* rearrangements (22, 57). The detection of any of these mutations indicates the presence of a malignant lesion, being the specificity greater than 96%, irrespective of the cytological diagnosis. However, the negative result harbors a low sensitivity (about 60%), and a large number of thyroid cancers can be missed. Very recently, a 167-gene expression classifier (16) has been subjected to a multicenter validation study demonstrating a high sensitivity (92%) and a high negative predictive value (95% for aspirates classified as atypia or follicular lesion of undetermined significance and 94% for follicular neoplasm or lesion suspicious for follicular neoplasm). This means that it only rarely misclassifies patients with malignant features as being healthy. Therefore, if the goal is ruling out malignancy and avoiding surgery, a similar approach is to be preferred. Despite the effectiveness in identifying truly negative lesions, this testing turned out to have a low specificity (52%), which still limits its usefulness in case of suspicious results. Thus, the development of new gene expression classifiers harboring a higher specificity is needed. In this setting, our experimental model may provide new insights to better distinguish benign from malignant thyroid nodules, based on gene expression clustering. Moreover, this approach may also prove useful for other purposes, such as for identifying prognostic genes and tailoring new targeted therapies. In conclusion, establishment of an enriched panel of molecular biomarkers, using data coming from mouse thyroid tumors and

validated in human specimens, may help to set up a more valid platform to further improve diagnosis and prognosis of thyroid malignancies.

Acknowledgments

Address all correspondence and requests for reprints to: Professor Giuseppe Damante, Dipartimento di Scienze Mediche e Biologiche, Piazzale Kolbe 1, 33100 Udine, Italy. E-mail: giuseppe.damante@uniud.it.

This work was supported by grants from the Associazione Italiana per la Ricerca sul Cancro (Grant IG 10296), the Ministero dell'Istruzione, dell'Università e della Ricerca (Grant 20093WAPYK_003), the Fondazione Umbero Di Mario, and the Banca d'Italia (to G.D.) and by National Institutes of Health Grant CA128943 (to A.D.C.). A.D.C. is also a recipient of the Irma T. Hirschl Career Scientist Award.

Disclosure Summary: The authors have nothing to disclose.

References

1. **Bartkova J, Horejsí Z, Koed K, Kräet al.** DNA damage response as a candidate anti-cancer barrier in early human tumorigenesis. *Nature*. 2005;434:864–870.
2. **Gorgoulis VG, Vassiliou LV, Karakaidos P, et al.** Activation of the DNA damage checkpoint and genomic instability in human precancerous lesions. *Nature*. 2005;434:907–913.
3. **Macaluso M, Paggi MG, Giordano A.** Genetic and epigenetic alterations as hallmarks of the intricate road to cancer. *Oncogene*. 2003; 22:6472–6478.
4. **Rennstam K, Hedenfalk I.** High-throughput genomic technology in research and clinical management of breast cancer. Molecular signatures of progression from benign epithelium to metastatic breast cancer. *Breast Cancer Res*. 2006;8:213.
5. **Hay ID, Klee GG.** Thyroid cancer diagnosis and management. *Clin Lab Med*. 1993;13:725–734.
6. **Eszlinger M, Krohn K, Hauptmann S, Dralle H, Giordano TJ, Paschke R.** Perspectives for improved and more accurate classification of thyroid epithelial tumors. *J Clin Endocrinol Metab*. 2008;93: 3286–3294.
7. **Caria P, Vanni R.** Cytogenetic and molecular events in adenoma and well-differentiated thyroid follicular-cell neoplasia. *Cancer Genet Cytogenet*. 2010;203:21–29.
8. **Marques AR, Espadinha C, Catarino AL, et al.** Expression of PAX8-PPARγ1 rearrangements in both follicular thyroid carcinomas and adenomas. *J Clin Endocrinol Metab*. 2002;87:3947–3952.
9. **Nikiforov YE, Nikiforova MN.** Molecular genetics and diagnosis of thyroid cancer. *Nat Rev Endocrinol*. 2011;7:569–580.
10. **Bruni P, Boccia A, Baldassarre G, Trapasso F, et al.** PTEN expression is reduced in a subset of sporadic thyroid carcinomas: evidence that PTEN-growth suppressing activity in thyroid cancer cells mediated by p27kip1. *Oncogene*. 2000;19:3146–3155.
11. **Gimm O, Perren A, Weng LP, et al.** Differential nuclear and cytoplasmic expression of PTEN in normal thyroid tissue, and benign and malignant epithelial thyroid tumors. *Am J Pathol*. 2000;156: 1693–1700.
12. **Tell G, Pines A, Arturi F, et al.** Control of PTEN gene expression in normal and neoplastic thyroid cells. *Endocrinology*. 2004;145: 4660–4666.
13. **Hou P, Liu D, Shan Y, et al.** Genetic alterations and their relationship in the phosphatidylinositol 3-kinase/Akt pathway in thyroid cancer. *Clin Cancer Res*. 2007;13:1161–1170.
14. **Xing M.** Genetic alterations in the phosphatidylinositol-3 kinase/Akt pathway in thyroid cancer. *Thyroid*. 2007;20:697–706.
15. **Knauf JA, Fagin JA.** Role of MAPK pathway oncoproteins in thyroid cancer pathogenesis and as drug targets. *Curr Opin Cell Biol*. 2009; 21:296–303.
16. **Alexander EK, Kennedy GC, Baloch ZW, et al.** Preoperative diagnosis of benign thyroid nodules with indeterminate cytology. *N Engl J Med*. 2012;367:705–715.
17. **Russo MA, Antico Arciuch VG, Di Cristofano A.** Mouse models of follicular and papillary thyroid cancer progression. *Front Endocrinol (Lausanne)*. 2011;2:119.
18. **Miller KA, Yeager N, Baker K, Liao XH, Refetoff S, Di Cristofano A.** Oncogenic Kras requires simultaneous PI3K signaling to induce ERK activation and transform thyroid epithelial cells in vivo. *Cancer Res*. 2009;69:3689–3694.
19. **Livak KJ, Schmittgen TD.** Analysis of relative gene expression data using real-time quantitative PCR and the 2[-ΔδC(T)] method. *Methods*. 2001;25:402–408.
20. **Puppin C, D'Aurizio F, D'Elia AV, et al.** Effects of histone acetylation on sodium iodide symporter promoter and expression of thyroid-specific transcription factors. *J Endocrinol*. 2005;146:3967–3974.
21. **Yeager N, Klein-Szanto A, Kimura S, Di Cristofano A.** Pten loss in the mouse thyroid causes goiter and follicular adenomas: insights into thyroid function and Cowden disease pathogenesis. *Cancer Res*. 2007;67:959–966.
22. **Cantara S, Capezzone M, Marchisotta S, et al.** Impact of proto-oncogene mutation detection in cytological specimens from thyroid nodules improves the diagnostic accuracy of cytology. *J Clin Endocrinol Metab*. 2010;95:1365–1369.
23. **Cheung L, Messina M, Gill A, et al.** Detection of the PAX8-PPARγ fusion oncogene in both follicular thyroid carcinomas and adenomas. *J Clin Endocrinol Metab*. 2003;88:354–357.
24. **Kubota T, Koshizuka K, Williamson EA, et al.** Ligand for peroxisome proliferator receptor γ (troglitazone) has potent effect against human prostate cancer both in vitro and in vivo. *Cancer Res*. 1998; 58:3344–3352.
25. **Chang TH, Szabo E.** Induction of differentiation and apoptosis by ligands of peroxisome proliferator-activated receptor γ in non-small cell lung cancer. *Cancer Res*. 2000;60:1129–1138.
26. **Kroll TG, Sarraf P, Pecciarini L, et al.** PAX8-PPARγ1 fusion oncogene in human thyroid carcinoma [corrected]. *Science*. 2000;289: 1357–1360.
27. **Funderburgh JL, Corpuz LM, Roth MR, Funderburgh ML, Tasheva ES, Conrad GW.** Mimecan, the 25-kDa corneal keratan sulfate proteoglycan, is a product of the gene producing osteoglycin. *J Biol Chem*. 1997;272:28089–28095.
28. **Long CJ, Roth MR, Tasheva ES, et al.** Fibroblast growth factor-2 promotes keratan sulfate proteoglycan expression by keratocytes in vitro. *J Biol Chem*. 2000;275:13918–13923.
29. **Shanahan CM, Cary NR, Osbourn JK, Weissberg PL.** Identification of osteoglycin as a component of the vascular matrix. Differential expression by vascular smooth muscle cells during neointima formation and in atherosclerotic plaques. *Arterioscler Thromb Vasc Biol*. 1997;17:2437–2447.
30. **Tasheva ES, Maki CG, Conrad AH, Conrad GW.** Transcriptional activation of bovine mimecan by p53 through an intronic DNA-binding site. *Biochim Biophys Acta*. 2001;1517:333–338.
31. **Wang Y, Ma Y, Lü B, Xu E, Huang Q, Lai M.** Differential expression of mimecan and thioredoxin domain-containing protein 5 in colorectal adenoma and cancer: a proteomic study. *Exp Biol Med (Maywood)*. 2007;232:1152–1159.
32. **Parton RG, Simons K.** The multiple faces of caveolae. *Nat Rev Mol Cell Biol*. 2007;8:185–194.
33. **Gustincich S, Vatta P, Goruppi S, et al.** The human serum depriva-

tion response gene (SDPR) maps to 2q32–q33 and codes for a phosphatidylserine-binding protein. *Genomics*. 1999;57:120–129.
34. **Li X, Jia Z, Shen Y, Ichikawa H, Jarvik J, Nagele RG, Goldberg GS.** Coordinate suppression of Sdpr and Fhl1 expression in tumors of the breast, kidney, and prostate. *Cancer Sci*. 2008;99:1326–1333.
35. **Kozak EM, Tate SS.** Glutathione-degrading enzymes of microvillus membranes. *J Biol Chem*. 1982;257:6322–6327.
36. **McIver CM, Lloyd JM, Hewett PJ, Hardingham JE.** Dipeptidase 1: a candidate tumor-specific molecular marker in colorectal carcinoma. *Cancer Lett*. 2004;209:67–74.
37. **Toiyama Y, Inoue Y, Yasuda H, et al.** DPEP1, expressed in the early stages of colon carcinogenesis, affects cancer cell invasiveness. *J Gastroenterol*. 2011;46:153–163.
38. **Austruy E, Cohen-Salmon M, Antignac C, et al.** Isolation of kidney complementary DNAs down-expressed in Wilms' tumor by a subtractive hybridization approach. *Cancer Res*. 1993;53:2888–2894.
39. **Green AR, Krivinskas S, Young P, et al.** Loss of expression of chromosome 16q genes DPEP1 and CTCF in lobular carcinoma in situ of the breast. *Breast Cancer Res Treat*. 2009;113:59–66.
40. **Schwanhäusser B, Busse D, Li N, et al.** Global quantification of mammalian gene expression control. *Nature*. 2011;473:337–342.
41. **Barden CB, Shister KW, Zhu B, et al.** Classification of follicular thyroid tumors by molecular signature: results of gene profiling. *Clin Cancer Res*. 2003;1792–1800.
42. **Aldred MA, Huang Y, Liyanarachchi S, et al.** Papillary and follicular thyroid carcinomas show distinctly different microarray expression profiles and can be distinguished by a minimum of five genes. *J Clin Oncol*. 2004;22:3531–3539.
43. **Chevillard S, Ugolin N, Vielh P, et al.** Gene expression profiling of differentiated thyroid neoplasms: diagnostic and clinical implications. *Clin Cancer Res*. 2004;10:6586–6597.
44. **Mazzanti C, Zeiger MA, Costouros NG, et al.** Using gene expression profiling to differentiate benign versus malignant thyroid tumors. *Cancer Res*. 2004;64:2898–2903.
45. **Cerutti JM, Delcelo R, Amadei MJ, et al.** A preoperative diagnostic test that distinguishes benign from malignant thyroid carcinoma based on gene expression. *J Clin Invest*. 2004;113:1234–1242.
46. **Finley DJ, Lubitz CC, Wei C, Zhu B, Fahey TJ 3rd.** Advancing the molecular diagnosis of thyroid nodules: defining benign lesions by molecular profiling. *Thyroid*. 2005;15:562–568.
47. **Weber F, Shen L, Aldred MA, et al.** Genetic classification of benign and malignant thyroid follicular neoplasia based on a three-gene combination. *J Clin Endocrinol Metab*. 2005;90:2512–2521.
48. **Hinsch N, Frank M, Döring C, Vorländer C, Hansmann ML.** QPRT: a potential marker for follicular thyroid carcinoma including minimal invasive variant; a gene expression, RNA and immunohistochemical study. *BMC Cancer*. 2009;9:93.
49. **Borup R, Rossing M, Henao R, et al.** Molecular signatures of thyroid follicular neoplasia. *Endocr Relat Cancer*. 2010;17:691–708.
50. **Griffith OL, Melck A, Jones SJ, Wiseman SM.** Meta-analysis and meta-review of thyroid cancer gene expression profiling studies identifies important diagnostic biomarkers. *J Clin Oncol*. 2006;24:5043–5051.
51. **Wang CC, Friedman L, Kennedy GC, et al.** A large multicenter correlation study of thyroid nodule cytopathology and histopathology. *Thyroid*. 2011;21:243–251.
52. **American Thyroid Association (ATA) Guidelines Task Force on Thyroid Nodules and Differentiated Thyroid Cancer, Cooper DS, Doherty GM, et al.** Revised American Thyroid Association management guidelines for patients with thyroid nodules and differentiated thyroid cancer. *Thyroid*. 2009;19:1167–1214.
53. **Bergenfelz A, Jansson S, Kristoffersson A, et al.** Complications to thyroid surgery: results as reported in a database from a multicenter audit comprising 3,660 patients. *Langenbecks Arch Surg*. 2008;393:667–673.
54. **Shrime MG, Goldstein DP, Seaberg RM, et al.** Cost-effective management of low-risk papillary thyroid carcinoma. *Arch Otolaryngol Head Neck Surg*. 2007;133:1245–1253.
55. **Russo D, Arturi F, Pontecorvi A, Filetti S.** Genetic analysis in fine needle aspiration biopsy of the thyroid: a new tool for the clinic. *Trends Endocrinol Metab*. 1999;10:280–285.
56. **Eszlinger M, Paschke R.** Molecular fine-needle aspiration biopsy diagnosis of thyroid nodules by tumor specific mutations and gene expression patterns. *Mol Cell Endocrinol*. 2010;322:29–37.
57. **Nikiforov YE, Ohori NP, Hodak SP, et al.** Impact of mutational testing on the diagnosis and management of patients with cytologically indeterminate thyroid nodules: a prospective analysis of 1056 FNA samples. *J Clin Endocrinol Metab*. 2011;96:3390–3397.